Supplementary Figures:

Movie S1: Division of an early embryo expressing PLK-1::sGFP and mCherry::HIS-11

Figure S1: PLK-1 is required for NEBD and localizes to the nuclear envelope in *C. elegans* oocytes and early embryos through its PBD domain

A- Differential interference contrast images (DIC) of the first embryonic division of **(a)** Wild-type and **(b)** *plk-1(or683*ts*)* embryos shifted for 2 hours to 25°C. Schematics summarize nuclear envelope dynamics. **(a)** In the Wild-type after fertilization, the female (pink) and the male (blue) pronuclei, which are surrounded by a nuclear envelope, meet at the posterior pole of the embryo. After rotation and centration of the nucleocentrosomal complex, the nuclear envelope breaks down in the vicinity of the centrosomes and between the juxtaposed pronuclei. This allows the capture of the chromosomes by the microtubules and the merging of the parental chromosomes in a single nucleus. **(b)** In *plk-1(or683*ts*)* embryos shifted 2-5 hours at 25°C, the nuclear envelope persists and physically separates the parental genomes during DNA segregation resulting in the formation of paired nuclei in each blastomere at the two-cell stage embryo.

B- (a) Confocal images of fixed Wild-type oocytes stained with PLK-1 antibodies (red) and counterstained with DAPI (blue). Scale bar, 2 μm. **(b, c)** Spinning disk confocal micrographs of oocytes expressing **(b)** PLK-1::sGFP or **(c)** GFP::PBD. Scale bar, 2 μm. (**d**) Confocal images of fixed Wild-type embryo at the pronuclei meeting stage stained with PLK-1 (red) and mAb414 (green) antibodies and counterstained with DAPI (blue). Scale bar, 5 μm.

C- Timing of PLK-1::sGFP recruitment to the NE (arrow) relative to NEBD defined as the time-point at which the nuclear envelope starts to deform (arrowhead) in P1 blastomere. Scale bar, 5μm. Note that the centrosomes are not always visible in the presented focal plane.

D- (**a**) Model of the tridimensional structure of the PLK-1 PBD. Residues H542 and K544 of the PB2 that contact the phosphopeptides and residue M547 that is mutated in the *plk-1*(*or683*ts*)* allele are presented and highlighted in green and purple, respectively. **(b)** Western blot analysis of budding yeast extracts expressing the indicated constructs using Gal4 DNA Binding Domain (DB) (upper panel) or Activation Domain (AD) antibodies (middle panels). Ponceau red staining of the membrane shows equal protein loading (bottom panel).

Figure S2: Genetic interactions between nucleoporins and *plk-1* hypomorphic allele

A- The schematic presents genetic interactions between NE components and the *plk-1(or683*ts*)* allele at 25°C. At this temperature, *plk-1(or683*ts*)* embryos present a penetrant paired nuclei phenotype as a result of defective NEBD. Down-regulation of certain NE components suppressed the paired nuclei phenotype of *plk-1(or683*ts*)*. The graph shows the percentage of *plk-1(or683*ts*)* embryos presenting 0 (green bars), 1 (orange bars) or 2 (red bars) paired nuclei at the two-cell stage upon exposure to the indicated RNAi at 25°C. The sample size (number of embryos analyzed) is provided in the figure and was generated by aggregation over 3 independent experiments.

B- The schematic shows the genetic assay used to search for nucleoporins whose inactivation enhanced the paired nuclei phenotype of hypomorphic *plk-1* alleles (*plk-1(or683*ts*)* at 15°C (upper panel) and *plk-1::sgfp* knock-in allele at 20°C (lower panel).

The graph shows the percentage of PLK-1::sGFP embryos presenting 0 (green bars), 1 (orange bars) or 2 (red bars) paired nuclei at the two-cell stage upon exposure to mock RNAi (*ctrl*), *npp-1*, *npp-4* or *npp-11(RNAi)* at 20°C. The sample size (number of embryos analyzed) is provided in the figure and was generated by aggregation over 3 independent experiments.

C- Western blot analysis of embryonic extracts from GFP::NPP-1 expressing strain exposed to RNAi treatments either mock (*ctrl*), *npp-1* or *npp-11* using GFP (upper panel), PLK-1 (middle panel) and tubulin (lower panel) antibodies.

D- Spinning disk confocal micrographs of 2-cell stage embryos expressing NPP-11::GFP after exposure to mock RNAi (*ctrl*), *npp-1, npp-4, npp-3* or *npp-13* RNAi. The graph shows the quantification of NPP-11::GFP signal intensity at the nuclear envelope in embryos of the indicated genotype. The sample size (number of embryos analyzed) is provided in the figure and was generated by aggregation over 3 independent experiments. The mean +/- standard error of the mean (sem) is presented. **** indicates statistically significant difference $p<0.0001$ with one-way ANOVA followed by Dunnett's multiple comparisons test.

Figure S3: Evolutionary conservation of Nup54/NPP-1, Nup58/NPP-4 and Nup62/NPP-11

Multiple protein alignments of Nup54, Nup58 and Nup62 from different species (*M. m: Mus musculus, R. n: Rattus norvegicus, H. s: Homo sapiens, X. t: Xenopus tropicalis, X. l: Xenopus Laevis, C. e: Caenorhabditis elegans, C. b: Caenorhabditis brenneri, C. r: Caenorhabditis remanei).* Sequences were aligned using Clustal W2 {Larkin et al., 2007, #10737} and visualized in Jalview {Waterhouse et al., 2009, #45561}. Sequence features were assigned based on the structural characterization of the Nup62•Nup58•Nup54 trimeric complex {Chug et al., 2015, #50942}. PBD-docking sites are underlined in red and structural determinants are indicated. CC : Coiled-coiled. The red stars mark aromatic residues, which are part of the heterotrimerization 2W3F coiled.

Figure S4: Cdk1 and PLK-1 phosphorylate nucleoporins to prime their interaction with the PLK-1 PBD

A- Full scans of Western blots corresponding to Figure 5B and 6A. Radioactive *in vitro* kinase assay was performed using human Cyclin B-Cdk1, or the *C. elegans* PLK-1 kinase, and GST (control), or the *C. elegans* NPP-1•NPP-4•NPP-11[C] (aa333-805) trimeric complex, as substrates. Autoradiograph of the SDS-PAGE showing γ-[^{32}P] incorporation in NPP-1, NPP-4 and NPP-11[C] (upper panel). Red asterisk marks autophosphorylated PLK-1. Coomassie brillant blue (CBB) staining of the same SDS-PAGE (bottom panel).

B- Full scans of Western blots corresponding to Figure 5C and 6B. *In vitro* kinase assay was performed with human Cyclin B-Cdk1 or the *C. elegans* PLK-1 kinase, and GST (control) or the *C. elegans* NPP-1•NPP-4•NPP-11[C] (aa333-805) trimeric complex as substrates. The samples were separated by SDS-PAGE followed by a Far-Western ligand-binding assay using GST-PBD Wild-type (upper panel) or the corresponding phosphate pincer (GST-PBD H538A/K540M) mutant (middle panel). Coomassie Brilliant Blue (CBB) staining shows protein loading of NPP-1•NPP-4•NPP-11[C] trimeric complex (bottom panel).

C- *In vitro* kinase assay was performed with human Cyclin B-Cdk1 and the NPP-1•NPP-11[C] dimer, or the NPP-1 4A (T8A, T49A, T60A, T105A)•NPP-11[C] 2A (T393A, T555A) dimer, or the NPP-1•NPP-4•NPP-11[C] trimer as substrates. The samples were separated by SDS-PAGE followed by a Far-Western ligand-binding assay using GST-PBD Wild-type (upper panel). Coomassie Brilliant Blue (CBB) staining (middle panel) and Western blot analysis (lower panel) show protein loading.

D- *In vitro* kinase assay was performed with human Cyclin B-Cdk1 and the 6xHis-NPP-11[C] (aa333-805) fragment, or the corresponding non-phosphorylatable 6xHis-NPP-11[C] (T555A), or 6xHis-NPP-11[C] 2A (T393A, T555A) variants as substrates. The samples were subjected to Phos-tag SDS-PAGE, followed by a Far-Western ligand-binding assay using the GST-PBD Wild-type. Western blot analysis using 6xHis antibodies reveals 6xHis-NPP-11[C] phosphorylated and non-phosphorylated fragments.

E- *In vitro* kinase assay was performed with human Cyclin B-Cdk1 or *C. elegans* PLK-1 kinase and NPP-19[N] (aa1-309) or the NPP-1•NPP-4•NPP-11[C] trimer as substrates. The samples were separated by SDS-PAGE followed by a Far-Western ligand-binding assay using GST-PBD Wild-type (upper panel) or the corresponding phosphate pincer (GST-PBD H538A/K540M) mutant (middle panel). Coomassie Brilliant Blue (CBB) staining shows protein loading (bottom panel).

Figure S5: Construction and phenotypic analysis of *npp-1* and *npp-11* deletion alleles removing the PBD-docking sites primed by Cdk1

A- Schematics of the *npp-1* (violet) and *npp-11* (blue) Wild-type and mutated genes and proteins with short deletions removing the PBD-docking sites primed by Cdk1. Vertical yellow bars indicate the position of the PBD-docking sites primed by Cdk1. The threonine T555 of NPP-11, which is outside the deleted region, was mutated to a non-phosphorylatable alanine (A) by CRISPR/Cas9. The region deleted in *npp-1* and *npp-11* is shaded in light violet and light blue, respectively. cc: coiled-coiled.

B- Western blot analysis of *C. elegans* embryonic extracts from Wild-type, *npp-1(syb207)* and *npp-11(ok1599It96)* alleles using Mab414 antibodies (upper panel). Ponceau staining of the membrane reveals equal protein loading (lower panel).

C- Representative spinning disk confocal micrographs of early embryos of the indicated genotype expressing **(a)** PLK-1::sGFP and mCherry::NPP-1 WT or **(b, c, d)** PLK-1::sGFP and mCherry::NPP-1 4A. White arrows show the persistence of the NE during anaphase. The white arrowhead indicates the persistence of the NE between the parental pronuclei.

Figure S6: Protein sequence of NPP-1, NPP-4 and NPP-11

The predicted PBD-docking sites primed by Cdk1 and PLK-1 are shaded in red and violet,

respectively, and other Cdk1-directed sites are shaded in green. Phenylalanine Glycine repeats (FG/GLF/GLFG/GGLFG) are shaded in yellow. The hetero-trimeric coiled-coiled promoting NPP-1•NPP-4•NPP-11 complex assembly is shaded in grey. The regions deleted in the *npp-1(syb207)* and *npp-11(ok1599It96)* alleles are underlined and bolded.

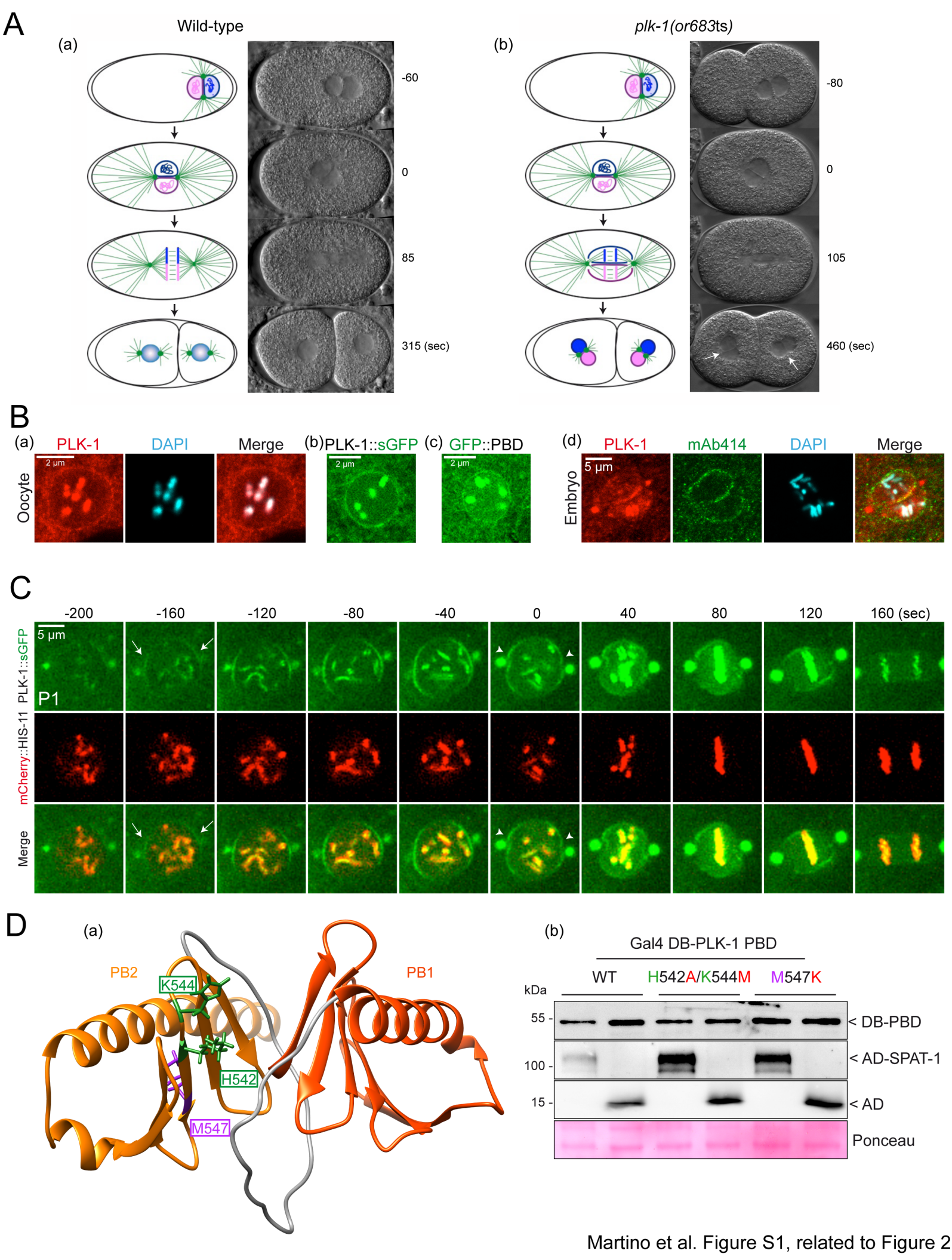

Martino et al. Figure S1, related to Figure 2

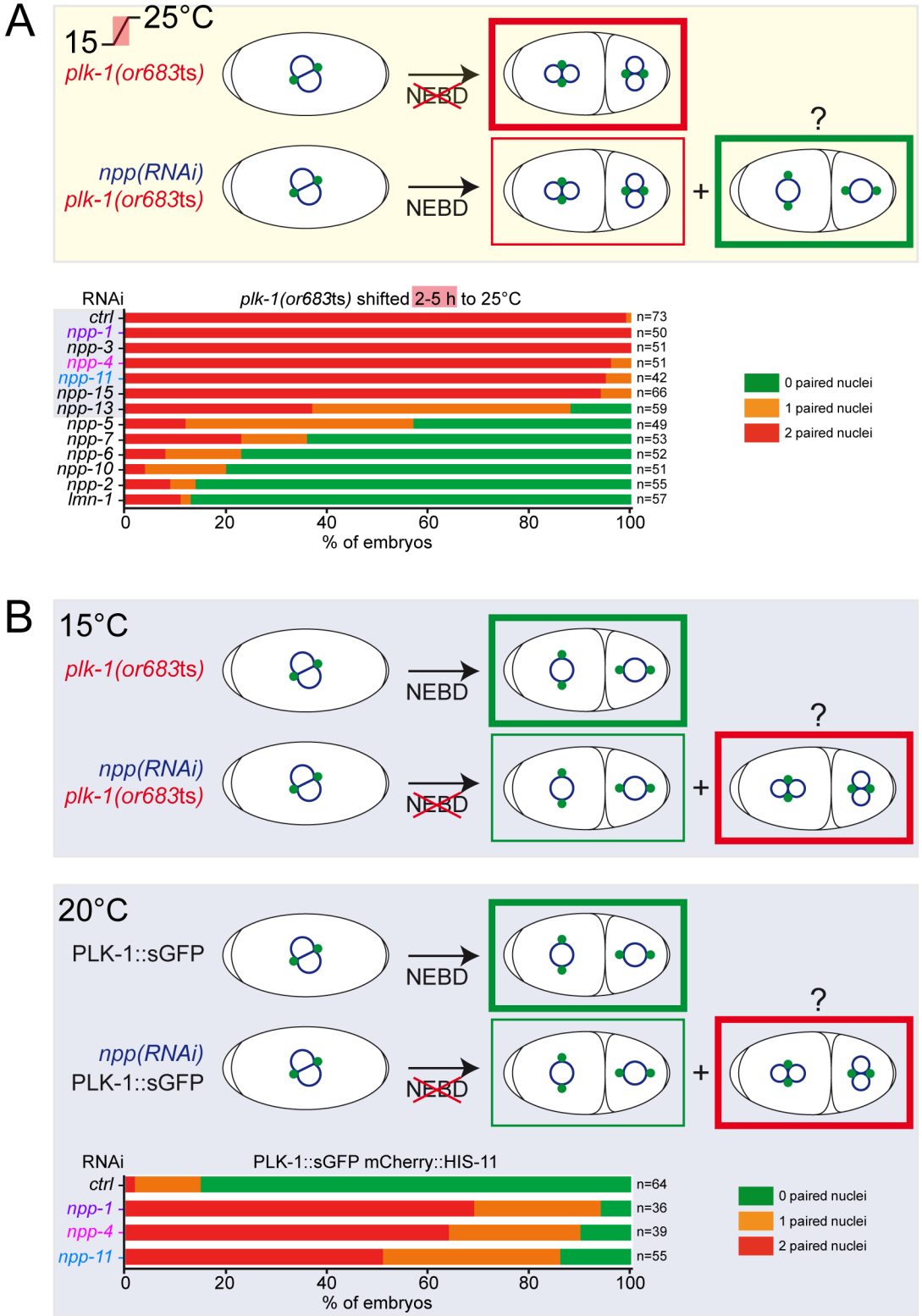

Martino et al. Figure S2, related to Figure 3

Nup54/NPP-1

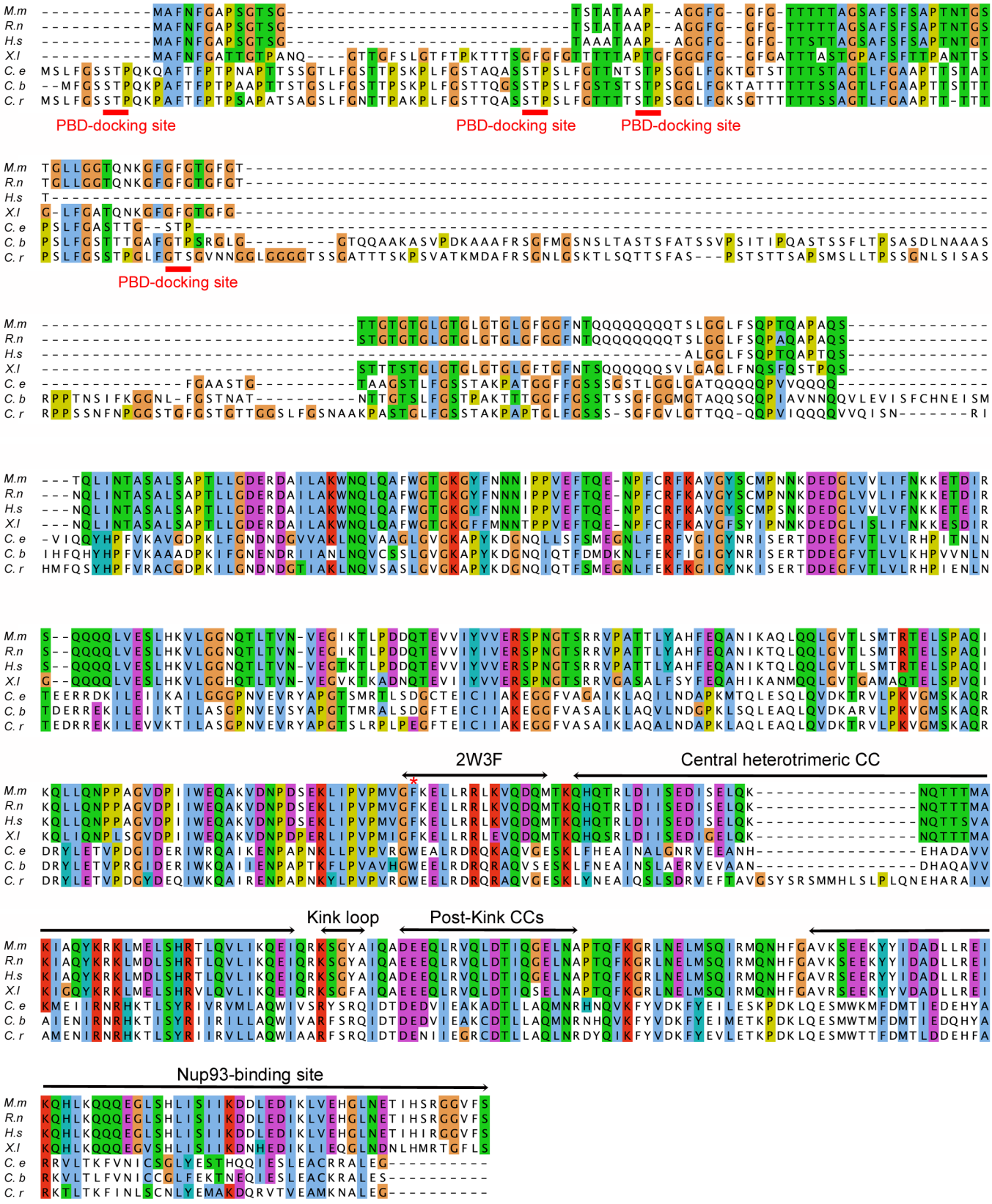
M.m
R.n
H.s
X.l
C. e
C. b
C. r
PBD-docking site
PBD-docking site
PBD-docking site
PBD-docking site
2W3F
Central heterotrimeric CC
Kink loop
Post-Kink CCs
Nup93-binding site

Nup58/NPP-4

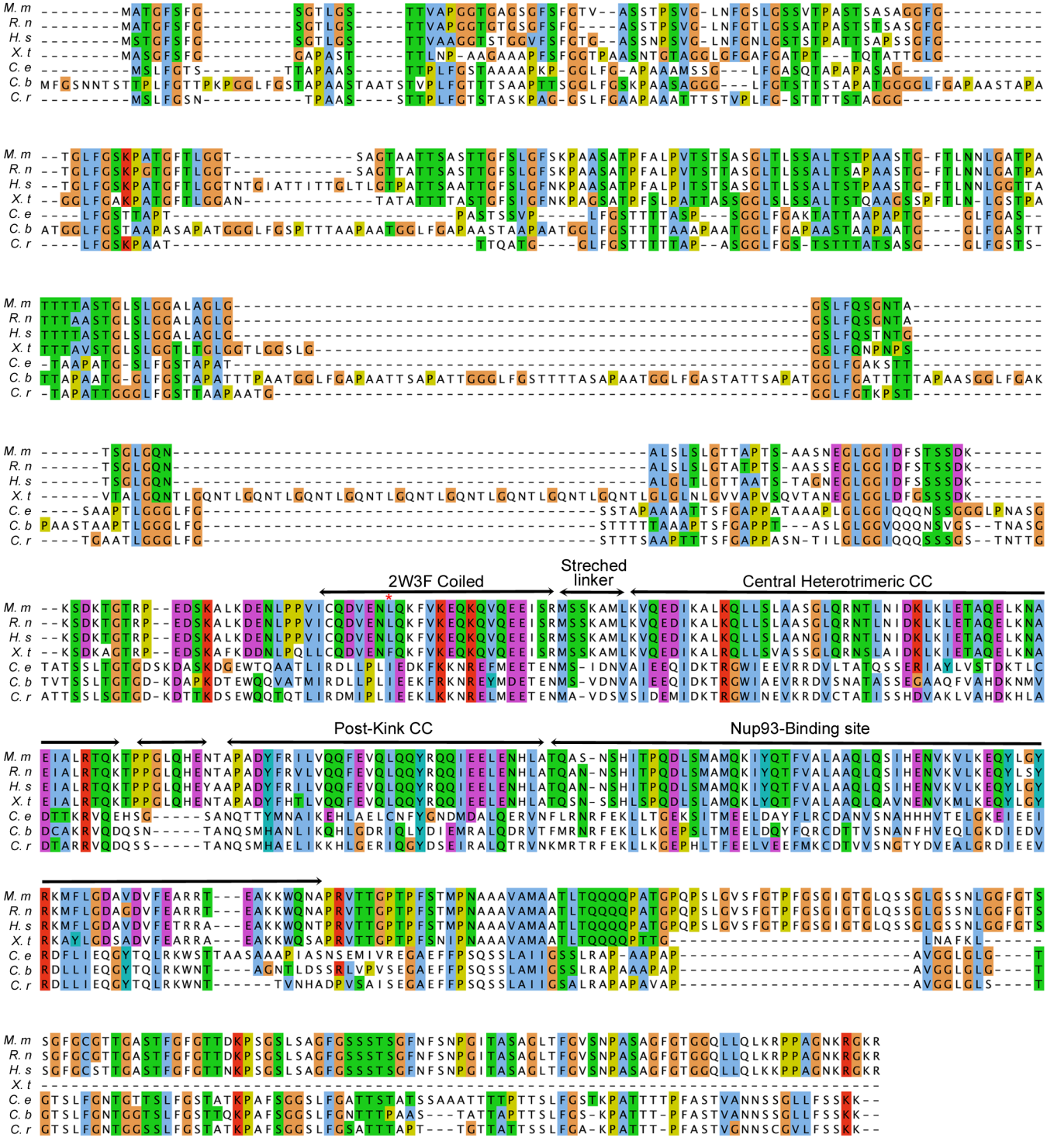
2W3F Coiled
Streched linker
Central Heterotrimeric CC
Post-Kink CC
Nup93-Binding site

Nup62/NPP-11

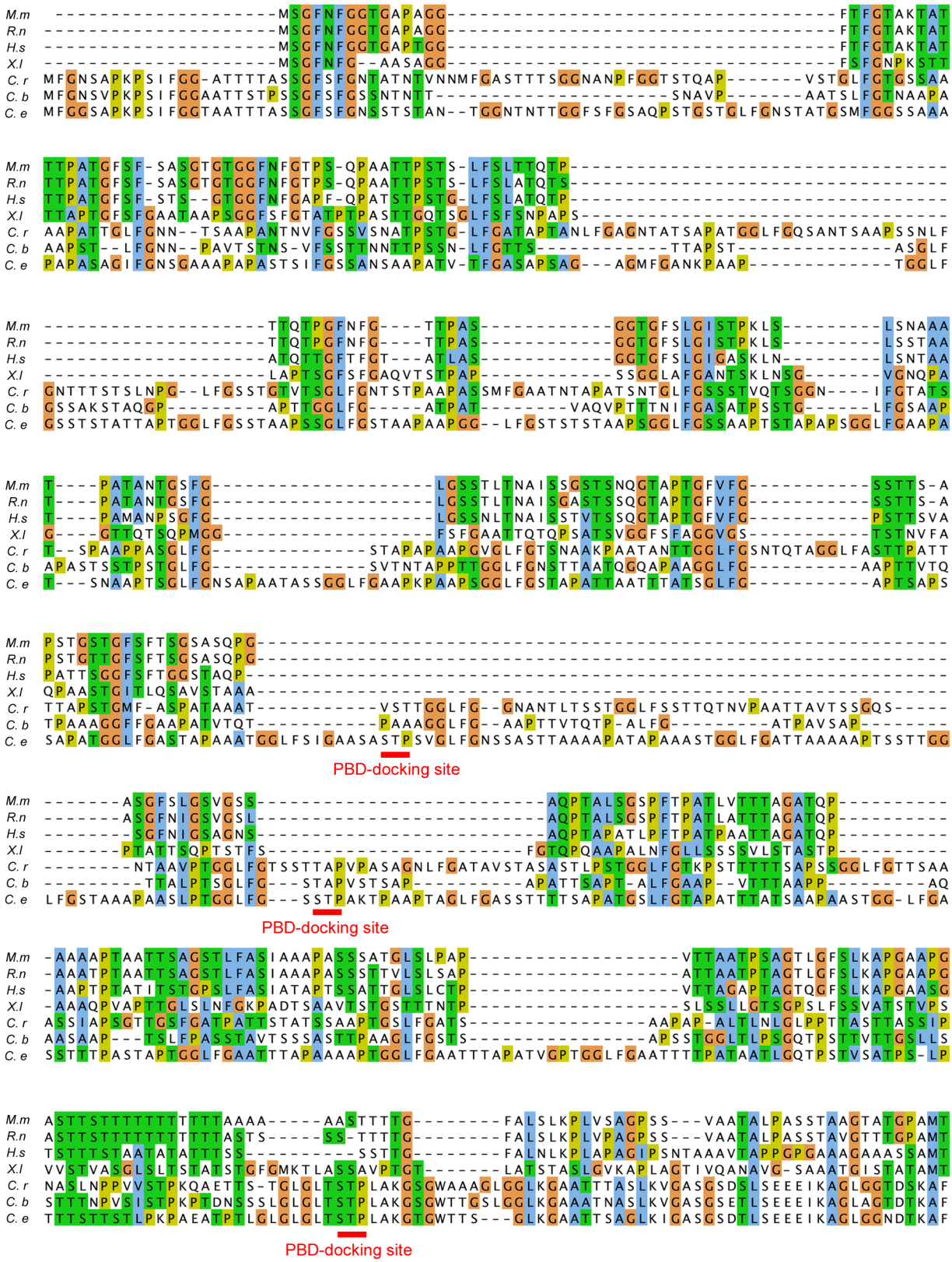
M.m
R.n
H.s
X.l
C. r
C. b
C. e
PBD-docking site
PBD-docking site
PBD-docking site

Nup62/NPP-11

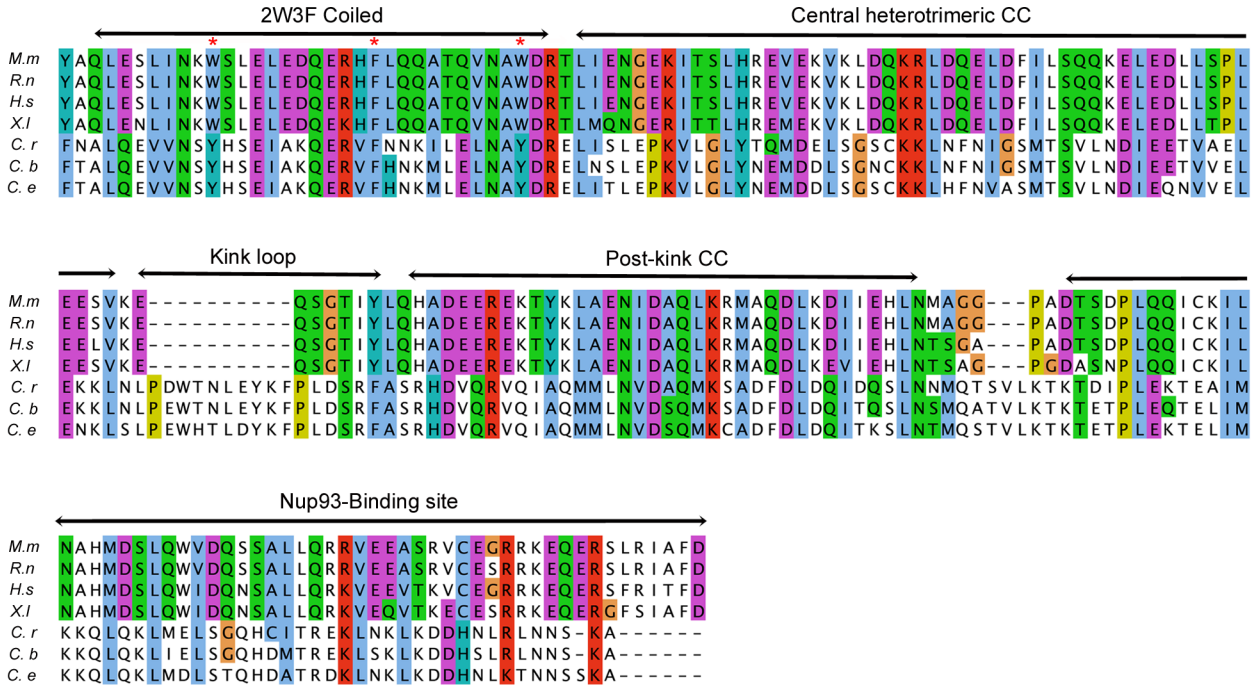

Martino et al Figure S3. 4/4

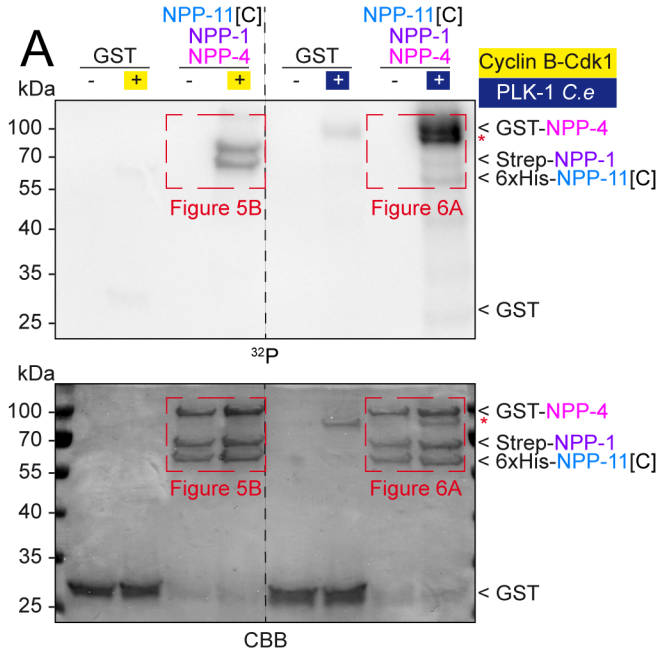

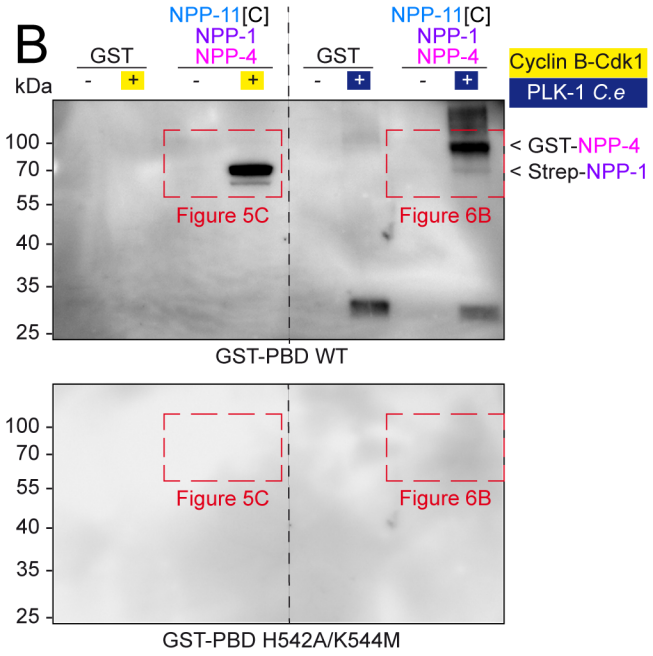

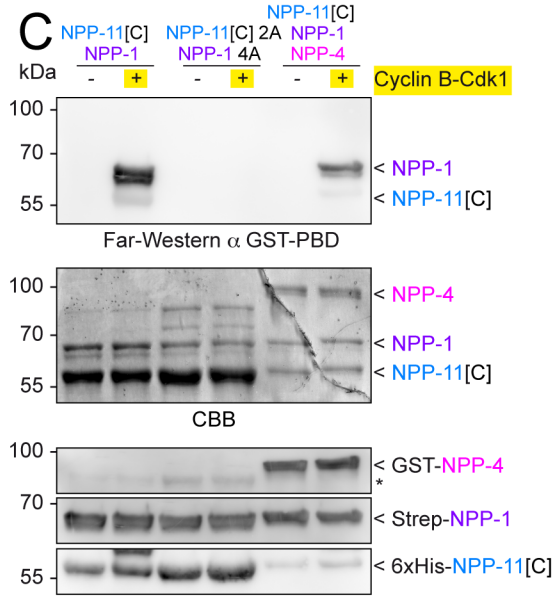

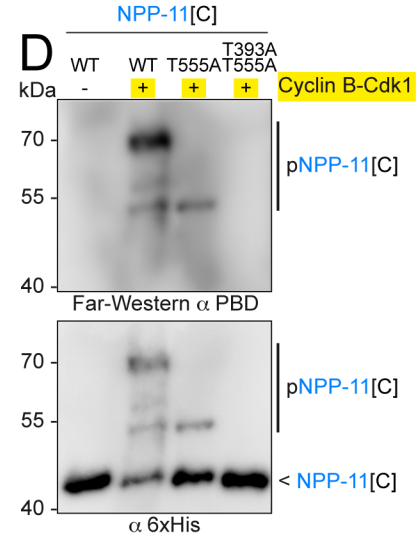

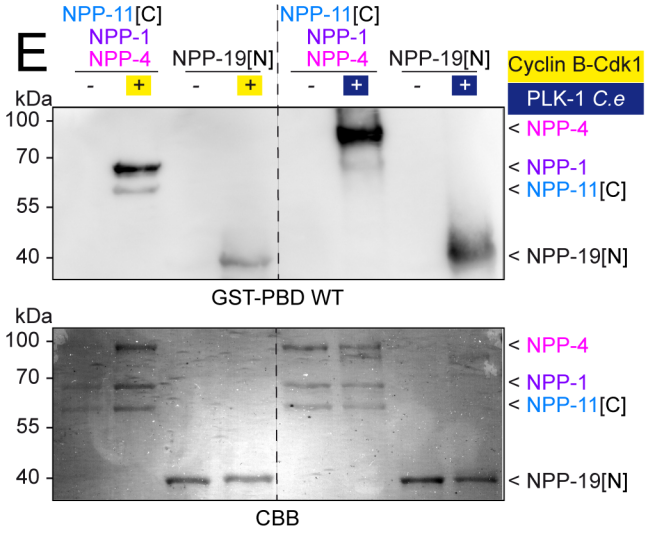

Martino et al. Figure S4, related to Figures 5 & 6

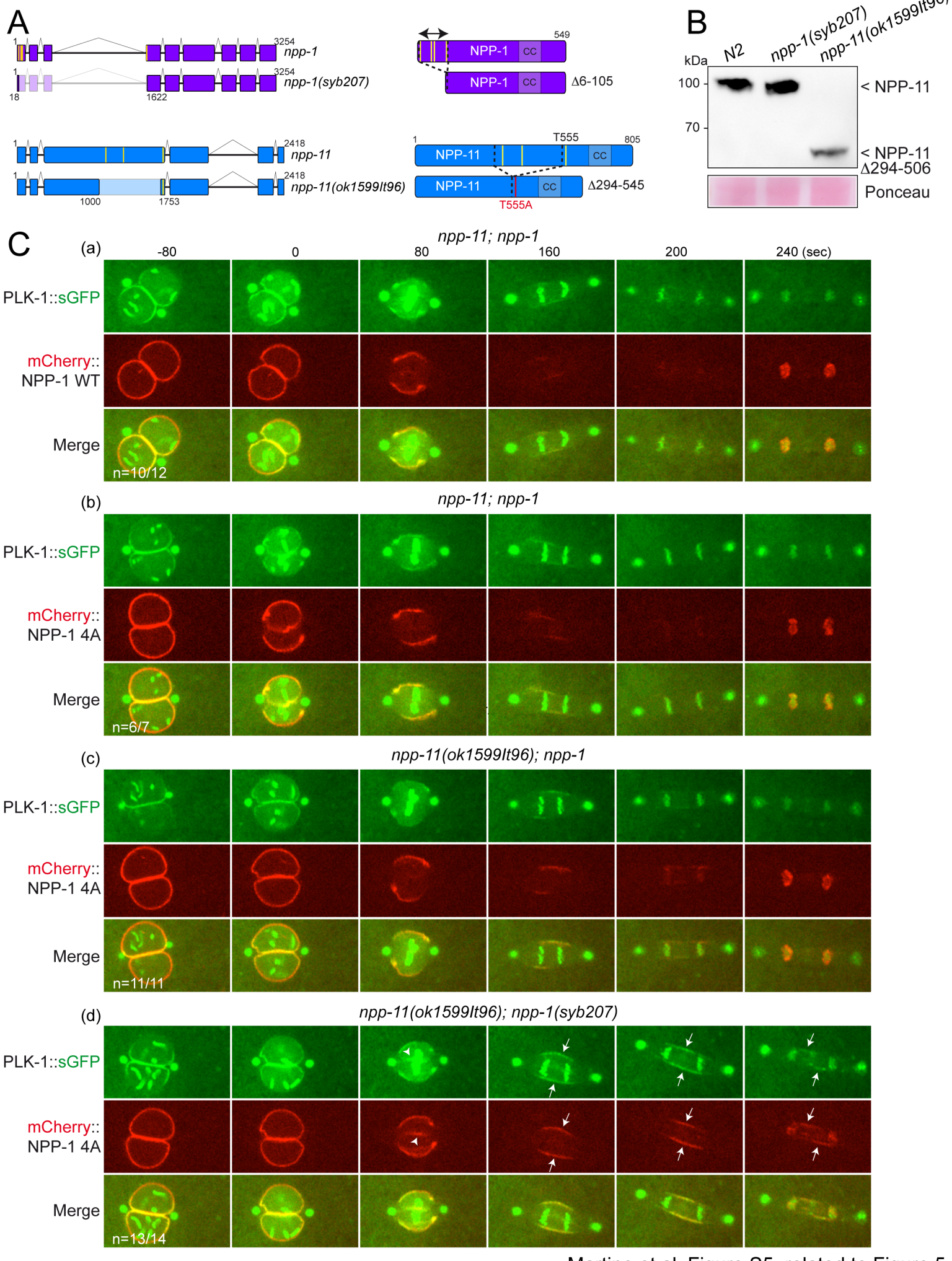

Martino et al. Figure S5, related to Figure 5

NPP-1

MSLFGSSTPQKQAFTFPTPNAPTTSSGTLFGSTTPSKPLFGSTAQASSTPSLFGTTNTSTPSGGLFGKTG
TSTTTTSTAGTLFGAAPTTSTATPSLFGASTTGSTPFGAASTGTAAGSTLFGSSTAKPATGGFFGSSSGS
TLGGLGATQQQQQPVVQQQQVIQQYHPFVKAVGDPKLFGNDNDGVVAKLNQVAAGLGVGKAPYKDGNQLL
SFSMEGNLFERFVGIGYNRISERTDDEGFVTLVLRHPITNLNTEERRDKILEIIKAILGGGPNVEVRYAP
GTSMRTLSDGCTEICIIAKEGGFVAGAIKLAQILNDAPKMTQLESQLQVDKTRVLPKVGMSKAQRDRYLE
TVPDGIDERIWRQAIKENPAPNKLLPVPVRGWEALRDRQKAQVGESKLFHEAINALGNRVEEANHEHADA
VVKMEIIRNRHKTLSYRIVRVMLAQWIVSRYSRQIDTDEDVIEAKADTLLAQMNRHNQVKFYVDKFYEIL
ESKPDKLQESMWKMFDMTIEDEHYARRVLTKFVNICSGLYESTHQQIESLEACRRALEG

NPP-4

MSLFGTSTTAPAASTTPLFGSTAAAAPKPGGLFGAPAAAMSSGLFGASQTAPAPASAGLFGSTTAPTPAS
TSSVPLFGSTTTTASPSGGLFGAKTATTAAPAPTGGLFGASTAAPATGSLFGSTAPATGGLFGAKSTTSA
APTLGGGLFGSSTAPAAAATTSFGAPPATAAAPLGLGGIQQQNSSGGGLPNASGTATSSLTGTGDSKDAS
KDGEWTQAATLIRDLLPLIEDKFKKNREFMEETENMSIDNVAIEEQIDKTRGWIEEVRRDVLTATQSSER
IAYLVSTDKTLCDTTKRVQEHSGSANQTTYMNAIKEHLAELCNFYGNDMDALQERVNFLRNRFEKLLTGE
KSITMEELDAYFLRCDANVSNAHHHVTELGKEIEEIRDFLIEQGYTQLRKWSTTAASAAAPIASNSEMIV
REGAEFFPSQSSLAIIGSSLRAPAAPAPAVGGLGLGTGTSLFGNTGTTSLFGSTATKPAFSGGSLFGATT
STATSSAAATTTTPTTSLFGSTKPATTTTPFASTVANNSSGLLFSSKK

NPP-11

MFGGSAPKPSIFGGTAATTTASSGFSFGNSSTSTANTGGNTNTTGGFSFGSAQPSTGSTGLFGNSTATGS
MFGGSSAAAPAPASAGIFGNSGAAAPAPASTSIFGSSANSAAPATVTFGASAPSAGAGMFGANKPAAPTG
GLFGSSTSTATTAPTGGLFGSSTAAPSSGLFGSTAAPAAPGGLFGSTSTSTAAPSGGLFGSSAAPTSTAP
APSGGLFGAAPATSNAAPTSGLFGNSAPAATASSGGLFGAAPKPAAPSGGLFGSTAPATTAATTTATSGL
FGAPTSAPSSAPATGGLFGASTAPAAATGGLFSIGAASASTPSVGLFGNSSASTTAAAAPATAPAAASTG
GLFGATTAAAAAPTSSTTGGLFGSTAAAPAASLPTGGLFGSSTPAKTPAAPTAGLFGASSTTTTSAPATG
SLFGTAPATTTATSAAPAASTGGLFGASSTTTPASTAPTGGLFGAATTTAPAAAAPTGGLFGAATTTAPA
TVGPTGGLFGAATTTTPATAATLGQTPSTVSATPSLPTTTSTTSTLPKPAEATPTLGLGLGLTSTPLAKG
TGWTTSGLKGAATTSAGLKIGASGSDTLSEEEIKAGLGGNDTKAFFTALQEVVNSYHSEIAKQERVFHNK
MLELNAYDRELITLEPKVLGLYNEMDDLSGSCKKLHFNVASMTSVLNDIEQNVVELENKLSLPEWHTLDY
KFPLDSRFASRHDVQRVQIAQMMLNVDSQMKCADFDLDQITKSLNTMQSTVLKTKTETPLEKTELIMKKQ
LQKLMDLSTQHDATRDKLNKLKDDHNLKTNNSSKA

S-Sp/Tp-P	Polo-docking sites primed by Cdk1
S-Sp/Tp	Polo-docking sites possibly primed by Plk1
Sp/Tp-P	Cdk1-consensus sites
FG/GLF/GLFG/GGLFG	FG repeats
Hetero-trimeric coiled-coiled	promoting NPP-1•NPP-4•NPP-11 complex assembly
Bold :	Region deleted in the *npp-1(syb207)* and *npp-11(ok1599It96)* alleles

Martino et al. Figure S6, related to Figure 5 & 6